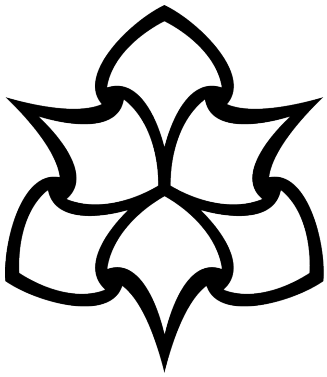

IEEE Access
Multidisciplinary | Rapid Review | Open Access Journal

Received February 8, 2020, accepted March 1, 2020, date of publication March 11, 2020, date of current version March 24, 2020.

Digital Object Identifier 10.1109/ACCESS.2020.2980171

Physical Layer Security of Cooperative NOMA for IoT Networks Under I/Q Imbalance

XINGWANG LI[1], (Senior Member, IEEE), MENGLE ZHAO[1], XIANG-CHUAN GAO[2], LIHUA LI[3], DINH-THUAN DO[4], (Senior Member, IEEE), KHALED M. RABIE[5], (Member, IEEE), AND RUPAK KHAREL[6], (Senior Member, IEEE)

[1]School of Physics and Electronic Information Engineering, Henan Polytechnic University, Jiaozuo 454003, China
[2]School of Information Engineering, Zhengzhou 450001, China
[3]State Key Laboratory of Networking and Switching Technology, Beijing University of Posts and Telecommunications, Beijing 100876, China
[4]Wireless Communications Research Group, Faculty of Electrical and Electronics Engineering, Ton Duc Thang University, Ho Chi Minh 700000, Vietnam
[5]Department of Engineering, Manchester Metropolitan University, Manchester M1 5GD, U.K.
[6]Department of Computing and Mathematics, Manchester Metropolitan University, Manchester M15 6BH, U.K.

Corresponding author: Xiangchuan Gao (iexcgao@zzu.edu.cn)

This work was supported in part by the Henan Scientific and Technological Research Project under Grant 182102210307, in part by the Key Young Teachers Project of Henan Province under Grant 2018GGJS006, in part by the key scientific research projects of colleges and universities in Henan Province under Grant 20A510010 and Grant 20A510007, in part by Major Projects of Henan Province under Grant 161100210200, in part by the National Key Research and Development Program under Grant 2019QY0302, in part by the National Natural Science Foundation of China (NSFC) under Grant U1736107, in part by the Fundamental Research Funds for the Universities of Henan Province under Grant NSFRF180309, and in part by the Outstanding Youth Science Foundation of Henan Polytechnic University under Grant J2019-4.

ABSTRACT In this paper, we investigate the reliability and security of cooperative dual-hop non-orthogonal multiple access (NOMA) for internet-of-thing (IoT) networks, in which the transceivers consider a detrimental factor of in-phase and quadrature-phase imbalance (IQI). The communication between the source and destination is accomplished through a decode-and-forward (DF) relay in the presence of an eavesdropper. In order to characterize the performance of the considered system, exact analytical expressions for the outage probability (OP) and intercept probability (IP) are derived in closed-form. Furthermore, to better understanding the performance of the considered system, we further derive the asymptotic expressions of OP in the high signal-to-noise ratio (SNR) regime and IP at the high main eavesdropping ratio (MER) region. A large number of analysis and Monte Carlo simulation results show that the existence of IQI usually increases the corresponding OP and reduces the IP, which means that reduces the reliability of the system and improves the security. In addition, the provided results provide useful insights into the trade-off between reliability and security of secure cooperative communication systems.

INDEX TERMS Cooperative communication, in-phase and quadrature-phase imbalance, Internet-of-Things, physical layer security, non-orthogonal multiple access.

I. INTRODUCTION

A. BACKGROUND

With the rapid development of the Internet of Things (IoT), the fifth generation (5G) wireless networks need to provide massive connectivity of IoT devices to meet the demand of high spectral efficiency and low latency [1]. The traditional orthogonal multiple access (OMA) technology is difficult to meeting the requirements of the 5G systems, and the non-orthogonal multiple access (NOMA) technology, as a novel multiple-access technology, which can not only improve the capacity and the spectral efficiency of the system well, but also the device access quantity can be increased by multiple times [2]. Compared with the OMA technology, the dominant characteristic of NOMA is to allow multiple users to share the same time, frequency and space resources by power-domain multiplexing [3]. At the transmitter, all the information is processed according to superposition coding, and then successive interference cancellation (SIC) is carried out at the receiver can decode their own information successfully [4]. In addition to enhancing the system performance, NOMA technology guarantees the fairness of multi-user by appropriate power distribution scheduling [5].

The associate editor coordinating the review of this manuscript and approving it for publication was Zhenyu Zhou.

Cooperative communication is considered to be a promising technology in mobile communication networks, which can improve spectrum efficiency, power efficiency and expand network coverage [6]. NOMA based cooperative relay systems has been studied to further improve network performance [1], [7]–[12]. In [7], the authors proposed a cooperative NOMA scheme by utilizing the characteristic that users with good channel conditions can obtain the information of users with poor channel conditions in advance, which proved that the near user with better channel conditions can forward the information of the far user, acting as a relay. The reliability of cooperative NOMA system based on successive user relaying (SR) technology was investigated by deriving the outage probability (OP) and asymptotic ergodic capacity of the considered systems [8], and also proposed an optimize power allocation factor algorithm to improve the fairness between users. A buffer-aided relay selection scheme was studied by the authors in [1], which can significantly improved the throughput of the system and achieved the seamless transmission of NOMA and OMA in the relay network. In [9], the authors applied cooperative NOMA to cognitive radio network, which improved the spectral efficiency. The trade-off between energy efficiency and time delay of cooperative relay protection systems was studied in [10], where a fractional programming and control parameter-based Lyapunov optimization method was proposed to solve stochastic-based energy efficiency optimization problems. In addition, according to the way of relay nodes process the information of source nodes, it can be divided into several cooperative protocols, such as amplifying and forwarding (AF), decoding and forwarding (DF). The authors in [11] studied the outage performance of AF NOMA cooperative relay system and derived the asymptotic OP and diversity order. The effect of fading parameters and average channel coefficients on the system performance was investigated in [12] by deriving the OP and throughput of a cooperative NOMA network with DF relay over Nakagami-m fading channels.

Since the broadcast characteristic of wireless transmission, the IoT networks are more vulnerable to attack by illegal users, thus, wireless communication urgently requires a communication network with a higher degree of information security [13]. As the basis of communication networks, information security is showing unprecedented importance [14]. The conventional methods to ensure the security of wireless communication are to use encryption algorithms, which rely on complexity and time-consumption. The physical layer security (PLS) technology is based on the broadcast characteristics of wireless transmission and can realize the communication network security in the sense of information theory without key, which has received remarkable attention, e.g., see [15]–[17] and the references therein. The concept of PLS was originally proposed by Wyner in [15]. Then, the authors investigated the secrecy performance of a cooperative system with DF scheme over Rician fading channels in [16]. The secrecy performance of systems with multiple eavesdroppers under colluding and non-colluding scenarios was studied in [17], where the channel state information (CSI) of the considered systems is outdated.

Recently, adopting PLS in cooperative NOMA systems has also attracted some significant research attentions. In [18], the authors derived the closed expressions of secure outage probability (SOP) and strictly positive secrecy capacity (SPSC) of cooperative NOMA system under AF and DF relay modes, which verified that the secure performance of the system can be improved by using the optimal power allocation parameters. In [19], a new NOMA cooperative jamming scheme was proposed to improve the security of the communication system. The authors in [20] evaluated the security and reliability of downlink cooperative NOMA in cognitive networks. In view of the multiple-relay assisted NOMA system, there are three relay selection schemes, i.e., optimal single relay selection (OSRS) scheme, two-step single relay selection (TSRS) scheme and optimal dual relay selection (ODRS) scheme were proposed to studied the secrecy outage performance of the considered system [21]. In order to improve the secure performance of the system, the authors proposed a cooperative jamming strategy for confuse relays in [21], and verified that the transmission power and fading parameters have a certain impact on the secure performance. As a further advance, a novel two-stage secure relay selection (TSSRS) with NOMA was proposed to improve the capacity between the source and destination in [22], so as to protect the communication link from eavesdropping. In addition, information transmission security can also be achieved by adding artificial noise [23]. Therefore, the secrecy performance of the multiple-antenna NOMA systems was enhanced by using the artificial noise technology in [24].

A common characteristic of the aforementioned research works is that they all consider the ideal RF front-end, and ignored the related defects of the RF front-end. However, low-cost, low-power, and small-size direct-conversion transceivers inevitably suffer from RF front-end related imperfections in practical communication systems due to the mismatch of analog components and the non-ideal transceiver manufacturing, which limit the overall system performance [25]. A typical example of these defects is the in-phase and quadrature-phase imbalance(IQI). This imbalance refers to the amplitude and phase mismatch between the in-phase (I) and quadrature-phase (Q) branches of the transceiver, which leads to imperfection of image suppression and ultimately to the degradation to the performance of the communication systems [26]. With perfect I/Q matching, the transceiver's I and Q branches will have the same amplitude and 90° phase shift [27]. However, in actual applications, due to the unsatisfactory analog components used in the transceiver, IQI always exists in the direct-conversion transceiver.

In this context, several research works analyzed the performance of system with IQI [28]–[31]. More specifically, the outage performance of the AF cooperative systems under

IQI was studied by deriving the exact closed-form analytical expressions of the OP and ergodic capacity for the considered system in [28]. The authors of [29] investigated the impact of RF front-end IQI on the performance of based on space time block coding (STBC)-orthogonal frequency division multiplexing (OFDM) systems. Then, the impact of IQI and phase noise (PHN) on the beamforming of OFDM direct-conversion transceivers was analyzed in [30]. A novel relay authentication scheme was proposed in [31] to enhance the security of the cooperation systems by utilizing the presence of IQI at the transceivers. However, only a few works in the open literature studied the impact of IQI on the performance of NOMA-based wireless communication systems [32], [33]. Specifically, the authors discussed the OP of the single-carrier and multi-carrier and which proved that IQI would have a different effect on each user of NOMA-based system in the presence of IQI [32]. The impact of IQI on cooperative NOMA systems in [33] was studied by deriving the OP and ergodic sum rate (ESR).

B. MOTIVATIONS AND CONTRIBUTION

Although there are a large amount of research works on cooperative NOMA systems, PLS and IQI, to the best of our knowledge, there is no relevant research work that discussed the security and reliability based on the cooperative NOMA system in the presence of IQI. In the literature [32], [33], the authors studied the impact of IQI on the performance of the NOMA system, but the possibility of eavesdropping on the communication link was not considered due to the time-varying nature of the wireless channel. Motivated by the aforementioned discussions, in this work, we study the secure performance of NOMA systems in terms of OP and IP in the presence of IQI. The main contributions to this paper are summarized as follows:

- Considering IQI at both the transmitter (TX) and receiver (RX), we investigate the reliability and security of the cooperative NOMA networks by deriving the exact closed-form analytical expressions for OP and IP of the far and near users.
- In order to get deeper insights of the reliability for the considered system, the asymptotic behaviors for the OP in the high signal-to-noise ratio (SNR) region are derived.
- By introducing the main-to-eavesdropper ratio (MER), we derive the asymptotic IP in the high MER region. We demonstrate that there is a trade-off between the outage and intercept performance, and provide useful insights.

C. ORGANIZATION AND NOTATIONS

The rest of this paper is organized as follows: Section II presents the cooperative NOMA system under consideration and channel model in the presence of IQI. In Section III, we derive the exact closed-form analytical expressions of OP and IP for the considered system in order to investigate the reliability and security. Section IV provides the respective numerical results and performance evaluation discussions. Finally, conclusions of this paper is given in Section V.

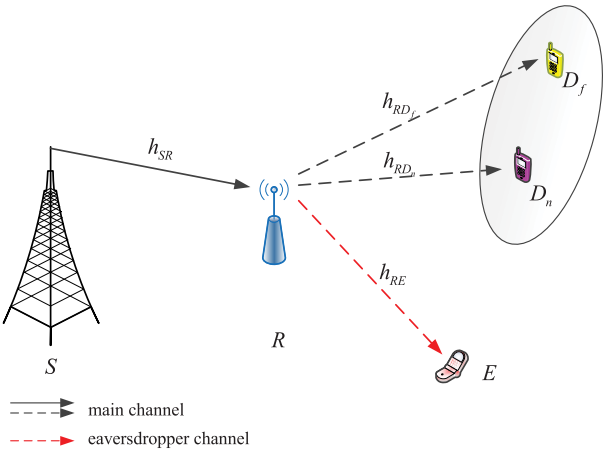

FIGURE 1. System model.

Notations: In this paper, the main notations are shown as follows: the $E\{\cdot\}$ and $|\cdot|$ denote the expectation and absolute operations, respectively. A complex Gaussian random variable with mean μ and variance σ^2 reads as $\mathcal{CN}\left\{\mu, \sigma^2\right\}$. $(\cdot)^*$ denotes conjugation. $\Re\{x\}$ and $\Im\{x\}$ represent the real and imaginary parts of x, respectively. Notation $Pr(\cdot)$ is the probability, while $f_x(\cdot)$ and $F_x(\cdot)$ are the probability density function (PDF) and the cumulative distribution function (CDF) of a random variable, respectively.

II. SYSTEM MODEL AND FADING MODEL

A. SYSTEM MODEL

We consider a downlink dual-hop underlay cooperative NOMA DF relay network shown in Fig. 1, which consists of one base station (BS) operating as the source (S), one relay (R), two legitimate destination nodes namely, the far user (D_f) and near user (D_n), and one eavesdropper (E), all nodes are equipped with a single antenna and have perfect CSI. On the premise of generality, we assume that there is no direct connection between S and destination, i.e., due to the large objects or heavy shadow, the source transmits the information to the destination node by the relay node. In addition, the E is only considered in the context of the R, it can intercept data from R.

Data transmission takes place in two phases, in the first phase, S transmits its information to R; in the second phase, R decodes and forwards the received signal to D and E. In this paper, we consider the existence of IQI on both the TX and the RX. In general, IQI is modeled as phase and/or amplitude imbalance between the transceiver I and Q signal paths. Therefore, the time-domain baseband representation of the IQI impaired signal is represented as [34]

$$x_{IQI} = \mu_{t/r} x + \nu_{t/r} x^*, \tag{1}$$

where x is the baseband transmitted signal under perfect TX/RX IQI matching, x^* indicates the mirror signal after being affected by IQI. In addition, the IQI coefficients $\mu_{t/r}$

and $\nu_{t/r}$ are given by [35]

$$\mu_t = \frac{1}{2}\left(1 + \varsigma_t \exp\left(j\phi_t\right)\right), \tag{2}$$

$$\nu_t = \frac{1}{2}\left(1 - \varsigma_t \exp\left(-j\phi_t\right)\right), \tag{3}$$

$$\mu_r = \frac{1}{2}\left(1 + \varsigma_r \exp\left(-j\phi_r\right)\right), \tag{4}$$

$$\nu_r = \frac{1}{2}\left(1 - \varsigma_r \exp\left(j\phi_r\right)\right), \tag{5}$$

where $\varsigma_{t/r}$ and $\phi_{t/r}$ denote the TX/RX amplitude and phase mismatch levels, respectively. It is noted that for ideal IQI, there parameters are $\varsigma_t = \varsigma_r = 1$, and $\phi_t = \phi_r = 0°$; in this case, we will get $\mu_t = \mu_r = 1$, $\nu_t = \nu_r = 0$.

1) The first phase: We assume an ideal RF front end, the transmitted signal at S represented as $x_s = \sqrt{a_1 P_s}x_1 + \sqrt{a_2 P_s}x_2$ with $E\left(|x_1|^2\right) = E\left(|x_2|^2\right) = 1$, where x_1 and x_2 are the transmitted signals from S for D_f and D_n, respectively; P_s is the transmit power at S; a_1 and a_2 are the power allocation coefficients with $a_1 + a_2 = 1$ and $a_1 > a_2$. We consider the existence of IQI on both the TX and the RF front-end, the received signal at the R is given by

$$y_R = \mu_{r_1}\left[h_1\left(\mu_{t_1}x_s + \nu_{t_1}(x_s)^*\right) + n_0\right] + \nu_{r_1}\left[h_1\left(\mu_{t_1}x_s + \nu_{t_1}(x_s)^*\right) + n_0\right]^*, \tag{6}$$

where h_1 is the small-scale fading coefficient between S and R, $n_0 \sim \mathcal{CN}(0, N_0)$ represents the complex additive white Gaussian noise (AWGN); μ_{t_1} and ν_{t_1} represent the amplitude and phase parameters of the IQI at the transmitter S, respectively; μ_{r_1} and ν_{r_1} are defined as the amplitude and phase parameters of the IQI at the transmitter R.

According to the NOMA protocol, SIC is applied at R to decode D_f's signal x_1 first and then cancel its component from the received signal to detect D_n's signal x_2. Thus, the received signal-to-interference-plus-noise ratio (SINR) of the signals x_1 and x_2 at R can be expressed as

$$\gamma_{SR}^{x_1} = \frac{a_1\rho_1\gamma_1 A_1}{a_2\rho_1\gamma_1 A_1 + \rho_1\gamma_1 B_1 + C_1}, \tag{7}$$

$$\gamma_{SR}^{x_2} = \frac{a_2\rho_1\gamma_1 A_1}{a_1\rho_1\gamma_1 D_1 + \rho_1\gamma_1 B_1 + C_1}, \tag{8}$$

where $A_1 = \left|\mu_{r_1}\mu_{t_1} + \nu_{r_1}\nu_{t_1}^*\right|^2$, $B_1 = \left|\mu_{r_1}\nu_{t_1} + \nu_{r_1}\mu_{t_1}^*\right|^2$, $C_1 = \left|\mu_{r_1}\right|^2 + \left|\nu_{r_1}\right|^2$, $D_1 = \left|\left(\mu_{r_1}\mu_{t_1} - 1\right) + \nu_{r_1}\nu_{t_1}^*\right|^2$, $\rho_1 = |h_1|^2$. In addition, we define $\gamma_1 = P_s/N_0$ as the transmit SNR at S. $A_1 = \left|\mu_{r_1}\mu_{t_1} + \nu_{r_1}\nu_{t_1}^*\right|^2 = \left|\mu_{r_1}\mu_{t_1}\right|^2 + \left|\nu_{r_1}\nu_{t_1}^*\right|^2 + 2\Re\left\{\mu_{r_1}\mu_{t_1}\nu_{r_1}\nu_{t_1}^*\right\}$, whereas due to the inequality [36]

$$2\Re\left\{\mu_{r_1}\mu_{t_1}\nu_{r_1}\nu_{t_1}^*\right\} \ll \left|\mu_{r_1}\mu_{t_1}\right|^2 + \left|\nu_{r_1}\nu_{t_1}^*\right|^2, \tag{9}$$

so A_1 can be accurately represented as $A_1 \approx \left|\mu_{r_1}\mu_{t_1}\right|^2 + \left|\nu_{r_1}\nu_{t_1}^*\right|^2$, in the same way $D_1 \approx \left|\mu_{r_1}\mu_{t_1} - 1\right|^2 + \left|\nu_{r_1}\nu_{t_1}^*\right|^2$.

2) The second phase: Use the DF protocol at R, the information transmitted from R is $x_R = \sqrt{b_1 P_R}x_1 + \sqrt{b_2 P_R}x_2$, where b_1 and b_2 are the power allocation coefficients with $b_1 + b_2 = 1$ and $b_1 > b_2$, P_R is the transmit power at R. Similarly, we consider that IQI exists at both the relay and the receiver, therefore, the received signals at D_f, D_n, and E can be respectively expressed as

$$y_{D_f} = \mu_{r_2}\left[h_2\left(\mu_{t_2}x_R + \nu_{t_2}(x_R)^*\right) + n_0\right] + \nu_{r_2}\left[h_2\left(\mu_{t_2}x_R + \nu_{t_2}(x_R)^*\right) + n_0\right]^*, \tag{10}$$

$$y_{D_n} = \mu_{r_3}\left[h_3\left(\mu_{t_2}x_R + \nu_{t_2}(x_R)^*\right) + n_0\right] + \nu_{r_3}\left[h_3\left(\mu_{t_2}x_R + \nu_{t_2}(x_R)^*\right) + n_0\right]^*, \tag{11}$$

$$y_E = \mu_{r_4}\left[h_4\left(\mu_{t_2}x_R + \nu_{t_2}(x_R)^*\right) + n_0\right] + \nu_{r_4}\left[h_4\left(\mu_{t_2}x_R + \nu_{t_2}(x_R)^*\right) + n_0\right]^*, \tag{12}$$

where h_2, h_3, h_4 are the channel coefficient between the $R \to D_f$, $R \to D_n$ and $R \to E$, respectively; μ_{t_2} and ν_{t_2} represent the amplitude and phase parameters of the IQI at the transmitter R, respectively; μ_{r_2} and ν_{r_2}, μ_{r_3} and ν_{r_3}, μ_{r_4} and ν_{r_4} are represented as IQI parameters at receiver D_f, D_n and E, respectively. The signals x_1 and x_2 are decoded and forwarded to D_f and D_n by R, respectively. The received SINR for D_f to decode the signal x_1 is given by

$$\gamma_{RD_f}^{x_1} = \frac{b_1\rho_2\gamma_2 A_2}{b_2\rho_2\gamma_2 A_2 + \rho_2\gamma_2 B_2 + C_2}, \tag{13}$$

where $A_i = \left|\mu_{r_i}\mu_{t_2} + \nu_{r_i}\nu_{t_2}^*\right|^2 \approx \left|\mu_{r_i}\mu_{t_2}\right|^2 + \left|\nu_{r_i}\nu_{t_2}^*\right|^2$, $B_i = \left|\mu_{r_i}\nu_{t_2} + \nu_{r_i}\mu_{t_2}^*\right|^2 \approx \left|\mu_{r_i}\nu_{t_2}\right|^2 + \left|\nu_{r_i}\mu_{t_2}^*\right|^2$, $C_i = \left|\mu_{r_i}\right|^2 + \left|\nu_{r_i}\right|^2$, $i \in (2, 3, 4)$, $\rho_i = |h_i|^2$. In addition, we define $\gamma_2 = P_R/N_0$ is the transmit average SNR at R.

Similarly, considering the perfect CSI of the D_n, the D_n will perform the SIC to cancel the interference caused by the D_f, which is generated under the assumption of perfect cancellation. Therefore, the received SINR at D_n can be given as

$$\gamma_{RD_n}^{x_1} = \frac{b_1\rho_3\gamma_2 A_3}{b_2\rho_3\gamma_2 A_3 + \rho_3\gamma_2 B_3 + C_3}, \tag{14}$$

$$\gamma_{RD_n}^{x_2} = \frac{b_2\rho_3\gamma_2 A_3}{b_1\rho_3\gamma_2 D_2 + \rho_3\gamma_2 B_3 + C_3}, \tag{15}$$

where $D_2 = \left|\left(\mu_{r_3}\mu_{t_2} - 1\right) + \nu_{r_3}\nu_{t_2}^*\right|^2 \approx \left|\mu_{r_3}\mu_{t_2} - 1\right|^2 + \left|\nu_{r_3}\nu_{t_2}^*\right|^2$.

According to the NOMA principle, E successfully eliminates the signal of D_f with SIC when the D_n's signal is eavesdropped and treats the signal of D_n as noise when the D_f's signal is eavesdropped. Thus, we can obtain

$$\gamma_E^{x_1} = \frac{b_1\rho_4\gamma_2 A_4}{b_2\rho_4\gamma_2 A_4 + \rho_4\gamma_2 B_4 + C_4}, \tag{16}$$

$$\gamma_E^{x_2} = \frac{b_2\rho_4\gamma_2 A_4}{b_1\rho_4\gamma_2 D_3 + \rho_4\gamma_2 B_4 + C_4}, \tag{17}$$

where $D_3 = \left|\left(\mu_{r_4}\mu_{t_2} - 1\right) + \nu_{r_4}\nu_{t_2}^*\right|^2 \approx \left|\mu_{r_4}\mu_{t_2} - 1\right|^2 + \left|\nu_{r_4}\nu_{t_2}^*\right|^2$.

B. STATISTICAL CHARACTERISTICS

In this paper, we assume that all channels experience Rayleigh fading [37]. ρ_i follows Rayleigh distribution with the PDF and CDF can be expressed as

$$f_{\rho_i}(x) = \frac{1}{\beta_i} e^{-\frac{x}{\beta_i}}, \tag{18}$$

$$F_{\rho_i}(x) = 1 - e^{-\frac{x}{\beta_i}}, \tag{19}$$

where $\beta_i = E[\rho_i]$ is the corresponding channel variance.

III. PERFORMANCE ANALYSES OF THE OUTAGE PROBABILITY AND INTERCEPT PROBABILITY

In this section, we investigate the reliability and security of the system by deriving the exact closed-form analytical expressions of the OP and IP. To obtain deeper insights, the asymptotic behaviors for the OP and IP are analyzed.

A. OUTAGE PROBABILITY ANALYSIS

1) Outage Probability for D_f

The outage event occurs at D_f when: i) R cannot successfully decode x_1 or x_2 and ii) R successfully decode x_1 and x_2 while D_f cannot decode its signal. Therefore, the OP at D_f can be represented as

$$P_{out}^{D_f} = 1 - \Pr\left(\min\left(\frac{\gamma_{x_1}^{SR}}{\gamma_{thf}}, \frac{\gamma_{x_2}^{SR}}{\gamma_{thn}}, \frac{\gamma_{x_1}^{RD_f}}{\gamma_{thf}}\right) > 1\right), \tag{20}$$

where γ_{thf} is the target rate of D_f.

Theorem 1: For Rayleigh fading channels, the exact closed-form expression for the OP of D_f is given by

$$P_{out}^{D_f} = 1 - e^{-\left(\frac{M_3}{\beta_1} + \frac{M_4}{\beta_2}\right)}, \tag{21}$$

where

$$M_1 = \frac{C_1\gamma_{thf}}{\gamma_1(a_1A_1 - a_2A_1\gamma_{thf} - B_1\gamma_{thf})},$$
$$M_2 = \frac{C_1\gamma_{thn}}{\gamma_1(a_2A_1 - a_1D_1\gamma_{thn} - B_1\gamma_{thn})},$$
$$M_4 = \frac{C_2\gamma_{thf}}{\gamma_2(b_1A_2 - b_2A_2\gamma_{thf} - B_2\gamma_{thf})},$$
$$M_3 = \max(M_1, M_2).$$

Moreover, (21) applies to the simultaneous establishment of

$$0 < \gamma_{thf} < \min\left(\frac{a_1A_1}{a_2A_1 + B_1}, \frac{b_1A_2}{b_2A_2 + B_2}\right), \tag{22}$$

and

$$0 < \gamma_{thn} < \frac{a_2A_1}{a_1D_1 + B_1}, \tag{23}$$

otherwise $P_{out}^{D_f} = 1$.

2) Outage Probability for D_n

The outage event occurs at D_n when: i) R can not successfully decode x_1 and x_2; ii) R decode x_1 and x_2 while D_n can not decode the signals. Therefore, the OP at D_n can be expressed as

$$P_{out}^{D_n} = \Pr\left(\min\left(\frac{\gamma_{x_1}^{SR}}{\gamma_{th,f}}, \frac{\gamma_{x_2}^{SR}}{\gamma_{th,n}}\right) < 1\right)$$
$$+ \Pr\left(\min\left(\frac{\gamma_{x_1}^{SR}}{\gamma_{th,f}}, \frac{\gamma_{x_2}^{SR}}{\gamma_{th,n}}\right) \geq 1, \min\left(\frac{\gamma_{x_1}^{RD_n}}{\gamma_{th,f}}, \frac{\gamma_{x_2}^{RD_n}}{\gamma_{th,n}}\right) < 1\right). \tag{24}$$

where γ_{thn} is the target rate of D_n.

Theorem 2: For Rayleigh fading channels, the exact closed-form expression for the OP of D_n is given by

$$P_{out}^{D_n} = 1 - e^{-\left(\frac{M_3}{\beta_1} + \frac{M_7}{\beta_3}\right)}, \tag{25}$$

where

$$M_5 = \frac{C_3\gamma_{thf}}{\gamma_2(b_1A_3 - b_2A_3\gamma_{thf} - B_3\gamma_{thf})},$$
$$M_6 = \frac{C_3\gamma_{thn}}{\gamma_2(b_2A_3 - b_1D_2\gamma_{thn} - B_3\gamma_{thn})},$$
$$M_7 = \max(M_5, M_6).$$

Note that all the conditions that make (25) happens if

$$0 < \gamma_{thf} < \min\left(\frac{a_1A_1}{a_2A_1 + B_1}, \frac{b_1A_3}{b_2A_3 + B_3}\right), \tag{26}$$

and

$$0 < \gamma_{thn} < \min\left(\frac{a_2A_1}{a_1D_1 + B_1}, \frac{b_2A_3}{b_1D_2 + B_3}\right), \tag{27}$$

otherwise $P_{out}^{D_n} = 1$.

Proof: See Appendix A. □

B. INTERCEPT PROBABILITY ANALYSIS

In this subsection, we analyze the secrecy performance of the cooperative NOMA system in the presence of IQI in terms of IP. The eavesdropper can successfully intercept the information of the legitimate user D_f or D_n only if the information of x_1 and x_2 is correctly decoded at R.

1) Intercept Probability for D_f

User D_f will be intercept if E can successfully wiretap D_f's signal. Then, the IP of D_f by E can be expressed as

$$P_{int}^{D_f} = \Pr\left(\gamma_{x_1}^{SR} > \gamma_{thf}, \gamma_{x_2}^{SR} > \gamma_{thn}, \gamma_{x_1}^{RE} > \gamma_{thE_1}\right), \tag{28}$$

where γ_{thE1} denotes the secrecy SNR threshold of D_f. The following theorem explores the secure performance in term of IP over Rayleigh fading channels with IQI.

Theorem 3: For Rayleigh fading channels, the exact closed-form expression for the IP of D_f is given by

$$P_{int}^{D_f} = e^{-\left(\frac{M_3}{\beta_1} + \frac{N_1}{\beta_4}\right)}, \tag{29}$$

where $N_1 = \frac{C_4\gamma_{thE_1}}{\gamma_2(b_1A_4 - b_2A_4\gamma_{thE_1} - B_4\gamma_{thE_1})}$ *with* $0 < \gamma_{thf} < \frac{a_1A_1}{a_2A_1+B_1}$, $0 < \gamma_{thn} < \frac{a_2A_1}{a_1D_1+B_1}$ *and* $0 < \gamma_{thE_1} < \frac{b_1A_4}{b_2A_4+B_4}$, *otherwise $P_{int}^{D_f} = 0$.*

2) Intercept Probability for D_n

$$P_{int}^{D_n} = \Pr\left(\gamma_{x_1}^{SR} > \gamma_{thf}, \gamma_{x_2}^{SR} > \gamma_{thn}, \gamma_{x_2}^{RE} > \gamma_{thE_2}\right), \tag{30}$$

where γ_{thE_2} denotes the secrecy SNR threshold of D_n. The following theorem explores the secure performance in term of IP over Rayleigh fading channels with IQI.

Theorem 4: For Rayleigh fading channels, the exact closed-form expression for the IP of D_n is given by

$$P_{int}^{D_n} = e^{-\left(\frac{M_3}{\beta_1}+\frac{N_2}{\beta_4}\right)}, \tag{31}$$

where $N_2 = \frac{C_4\gamma_{thE_2}}{\gamma_2(b_2A_4-b_1D_3\gamma_{thE_2}-B_4\gamma_{thE_2})}$ *with* $0 < \gamma_{thf} < \frac{a_1A_1}{a_2A_1+B_1}$, $0 < \gamma_{thn} < \frac{a_2A_1}{a_1D_1+B_1}$ *and* $0 < \gamma_{thE_1} < \frac{b_2A_4}{b_1D_3+B_4}$, *otherwise* $P_{int}^{D_n} = 0$.

Proof: See Appendix B. □

C. ASYMPTOTIC ANALYSIS

In order to obtain further insights, we focus on the asymptotic analysis in terms of OP and IP.

1) Outage Probability

At high SNRs, the CDF of the channel gain ρ_i can be expressed as

$$F_{\rho_i}^{\infty}(x) \approx \frac{x}{\beta_i}, \tag{32}$$

Corollary 1: At high SNRs, the asymptotic expression for the OP of D_f in cooperative NOMA system is given as

$$\begin{aligned} P_{out}^{D_f,\infty} &= F_{\rho_1}^{\infty}(M_3) + F_{\rho_2}^{\infty}(M_4) - F_{\rho_1}^{\infty}(M_3)\,F_{\rho_2}^{\infty}(M_4) \\ &= \frac{M_3}{\beta_1} + \frac{M_4}{\beta_2} - \frac{M_3M_4}{\beta_1\beta_2}. \end{aligned} \tag{33}$$

Corollary 2: At high SNRs, the asymptotic expression for the OP of D_n in cooperative NOMA system is given as

$$\begin{aligned} P_{out}^{D_n,\infty} &= F_{\rho_1}^{\infty}(M_3) + F_{\rho_2}^{\infty}(M_7) - F_{\rho_1}^{\infty}(M_3)\,F_{\rho_2}^{\infty}(M_7) \\ &= \frac{M_3}{\beta_1} + \frac{M_7}{\beta_3} - \frac{M_3M_7}{\beta_1\beta_3}. \end{aligned} \tag{34}$$

Remark 1: From ***Corollary 1*** *and* ***Corollary 2****, we can obtain that the asymptotic outage performance of the D_f and D_n changes with the average transmit SNR.*

2) Intercept Probability

Corollary 3: We taking the MER as $\beta_{me} = \beta_1/\beta_4$. *According to* $\exp(-x) \underset{x\to 0}{\approx} 1-x$, *at high MER, the asymptotic expression for the IP of D_f in cooperative NOMA system is given as*

$$\begin{aligned} P_{int}^{D_f,\infty} &= e^{-\frac{1}{\beta_4}\left(\frac{M_3}{\beta_{me}}+N_1\right)} \\ &\approx e^{-\frac{N_1}{\beta_4}}\left(1-\frac{M_3}{\beta_4\beta_{me}}\right). \end{aligned} \tag{35}$$

Corollary 4: At high MER, the asymptotic expression for the IP of D_n in cooperative NOMA system is given as

$$\begin{aligned} P_{int}^{D_n,\infty} &= e^{-\frac{1}{\beta_4}\left(\frac{M_3}{\beta_{me}}+N_2\right)} \\ &\approx e^{-\frac{N_2}{\beta_4}}\left(1-\frac{M_3}{\beta_4\beta_{me}}\right). \end{aligned} \tag{36}$$

IV. NUMERICAL RESULTS

In this section, some numerical results are given to validate the correctness of theoretical analysis of the OP and IP. The results are then verified using Monte Carlo simulations with 10^7 iterations. Unless otherwise specified, we have used the following parameter values: $N = 1$, $\gamma_{thf} = 1$, $\gamma_{thn} = 3$, $\gamma_{thE1} = \gamma_{thE2} = 2$, the power allocation coefficients are $a_1 = b_1 = 0.9$ and $a_2 = b_2 = 0.1$, the channel fading parameters are $\beta_1 = 1$, $\beta_2 = \beta_3 = 0.5$, $\beta_4 = 1$. Furthermore, the IQI parameters are set as $\varsigma_t = \varsigma_r = 1.1$, $\phi_t = \phi_r = 5°$, for the ideal RF front-end $\varsigma_t = \varsigma_r = 1$, $\phi_t = \phi_r = 0°$.

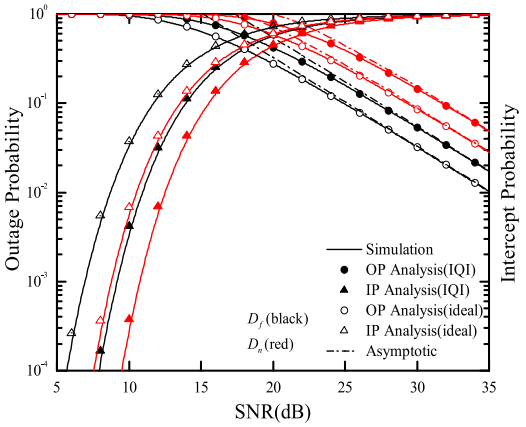

FIGURE 2. OP and IP versus the transmit SNR.

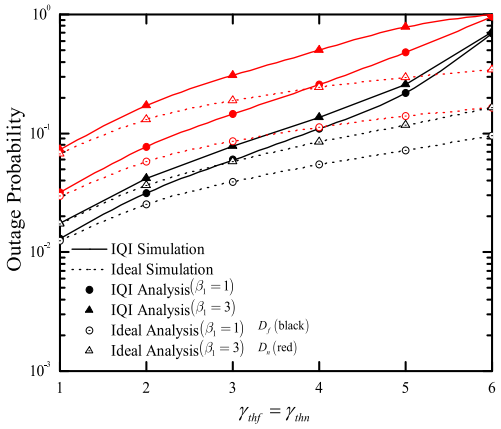

FIGURE 3. OP versus the target rate ($\gamma_{thf} = \gamma_{thn}$) for different β_1.

Fig. 2 shows the OP and IP of cooperative NOMA network versus the transmit SNR under the ideal and IQI conditions. These curves represent the OP, IP, and asymptotic analysis obtained from (21), (25), (29), (31) and (33), (34). From this figure, we can see that the theoretical analysis matches precisely with the Monte Carlo simulation results over the entire SNRs region, which verifies the correctness of our analysis. These results also indicate that the outage performance of each user under ideal conditions outperforms that of the IQI conditions, and the IP under ideal conditions is greater than that under IQI conditions, which means that the presence of IQI can reduce reduces the reliability and improve the security of the system. In addition, there is a trade-off between reliability and security, which implies that performance optimization is required.

Fig. 3 demonstrates the OP versus target rate for different fading parameters ($\beta_1 = 1, 3$) under ideal and IQI conditions. In this simulation, we set $SNR = 30$dB and assume that the far user and near user have the same target rate. From the Fig. 3, we can see that the user's OP increases with

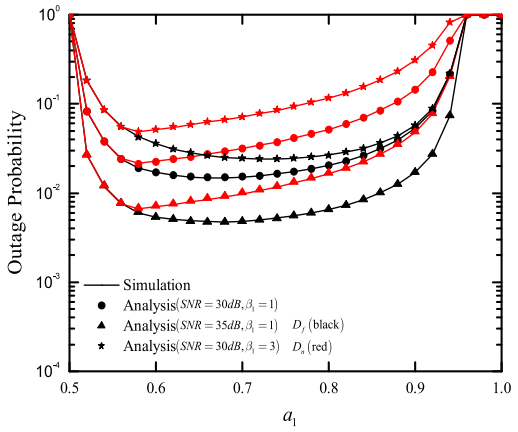

FIGURE 4. OP versus a_1 for different transmit SNR and β_1.

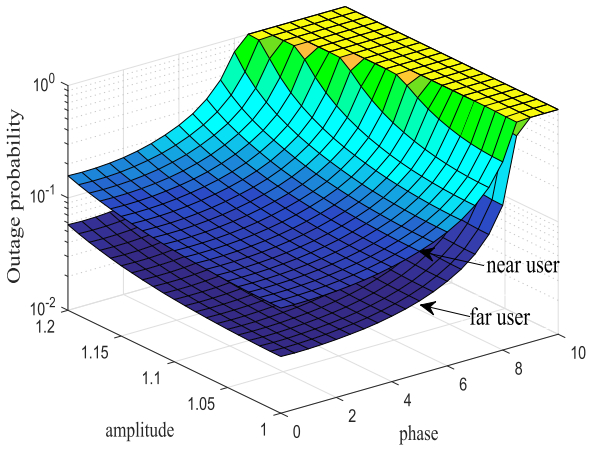

FIGURE 5. OP versus amplitude mismatch $(\varsigma_t = \varsigma_r)$ and phase mismatch $(\phi_t = \phi_r)$.

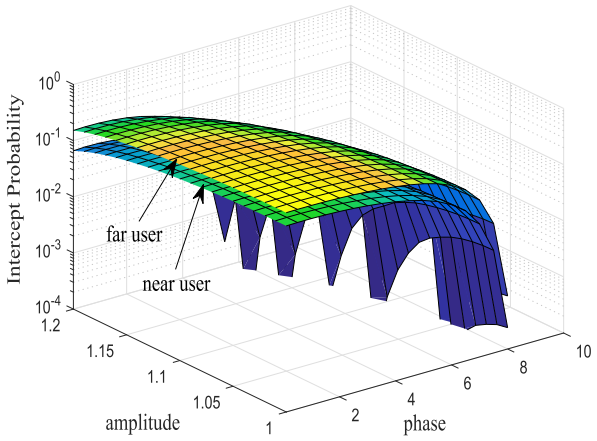

FIGURE 6. IP versus amplitude mismatch $(\varsigma_t = \varsigma_r)$ and phase mismatch $(\phi_t = \phi_r)$.

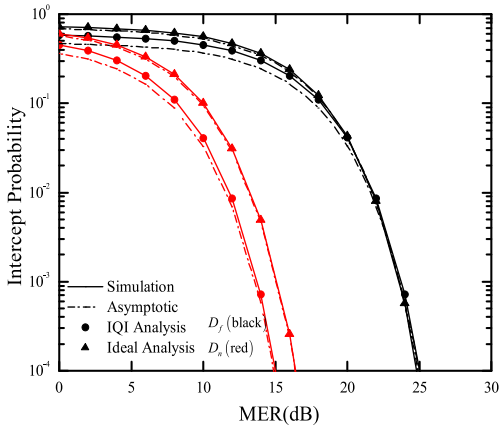

FIGURE 7. IP versus MER.

the increase of γ_{thf}. When the channel fading parameter β_1 increases, the reliability of the considered system increases. Furthermore, it is shown that IQI affects D_n more severely than D_f, which is due to the fact that D_n is also subjected to interference from D_f after the SIC is executed, which leads to the increase of OP.

Fig. 4 presents the OP versus the power allocation ratio a_1 for different transmit SNR values and fading parameters β_1. First of all, we can see that D_f is in an outage when $\gamma_{thf} > \min\{a_1A_1/(a_2A_1 + B_1), b_1A_2/(b_2A_2 + B_2)\}$ or $\gamma_{thn} > a_2A_1/(a_1D_1 + B_1)$, D_n is in an outage when $\gamma_{thf} > \min\{a_1A_1/(a_2A_1 + B_1), b_1A_3/(b_2A_3 + B_3)\}$ or $\gamma_{thn} > \min(a_2A_1/(a_1D_1 + B_1), b_2A_3/(b_1D_2 + B_3))$. In other cases, these curves first decrease and then increase as a_1 increases. As a matter of fact, the larger a_1 is, the easier it becomes to decode x_1, and the decoding of x_2 becomes more difficult, hence the combination of x_1 and x_2 causes a change in the curves. Furthermore, we can also see that no matter how SNR and β_1 change, D_n always has an optimal performance value when $a_1 \approx 0.57$, while the change of *SNR* has a slight effect on the optimal value of D_f, and the change of β_1 has great influence on the optimal value of D_f.

Fig. 5 depicts the OP of the far and near users versus the amplitude mismatch $(\varsigma_t = \varsigma_r)$ and phase mismatch $(\phi_t = \phi_r)$. Note that in these results, we set $SNR = 30$dB. We can see that for a certain phase, when the amplitude increases, the change of the OP for far user and near user is less pronounced. For a certain amplitude, the OP of far user and near user increases significantly with the increase of phase. This phenomenon indicates that the reliability of the system is more sensitive to phase mismatch than it is to the amplitude mismatch. That is, the outage performance of D_f and D_n is broken as ς_t and ϕ_t increases.

Fig. 6 shows IP versus phase mismatch $(\phi_t = \phi_r)$ and phase mismatch $(\phi_t = \phi_r)$. Note that in these results, we set $SNR = 15$dB. This figure indicates that the effect of amplitude mismatch and phase mismatch on IP is opposite to the OP, which means that amplitude mismatch and phase mismatch parameters can improve the secure performance of the system. In general, Fig. 5 and Fig. 6 provide a rough estimate of the maximum IQI level, and the cooperative communication system can withstand to achieve the desired reliability and security. Therefore, it can help when designing communication systems to combat undesired IQI effects.

Fig. 7 presents the IP of a cooperative NOMA system versus MER with $SNR = 20$dB. For this case, we analyze the IP and asymptotic expressions of far user and near user

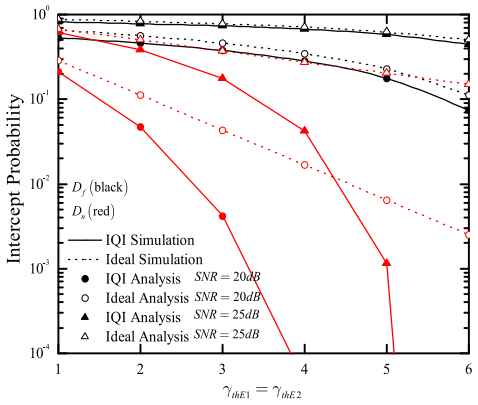

FIGURE 8. IP versus the target rate $\gamma_{thE_1} = \gamma_{thE_2}$ for different transmit *SNR*.

at E. It is obvious that the asymptotic expressions are strict approximation of the exact IP and the IQI effects reduced the IP of the NOMA users. We can also observe that the impact of IQI on each NOMA user is different. In this figure, we consider E performs perfect SIC, however, if E does not know the order of the users in advance, SIC will not be possible. In this case, E cannot intercept the D_n's signal because the D_f allocates more power than the D_n.

Fig. 8 illustrates the IP versus the target rate for different transmit SNR values. For this figure, we set $MER = 5$dB and assume that the D_f and D_n have the same target rate. One can observe that the IP of $SNR = 25$dB is better than that of $SNR = 20$dB. In addition, we can also observe that the presence of IQI has a small impact on D_f, but has a great impact on D_n.

V. CONCLUSION

In this paper, we investigate the effects of IQI on the reliability and security for cooperative NOMA enabled IoT networks over Rayleigh fading channels. The practical factor of IQI at TX and RX are considered insightfully. Specifically, we derive the closed-form analytical expressions of the OP and IP for the far user and near user under IQI, and analyze the asymptotic OP in the high SNR region and the asymptotic IP in the high MER regime. The results obtained have been verified by Monte Carlo simulation. These results show that as the amplitude and phase parameters of the IQI increase, the user's OP increases, and the IP decreases. The user's OP decreases first and then increases as the power allocation parameter a_1 increases, that is, the performance of considered system is optimal when $a_1 \approx 0.57$. In addition, the severity of the performance degradation depends on several factors, including the power allocation ratio, the transmission SNR ratio, and the order of considered users.

APPENDIX A: PROOF OF THEOREM 1

1) Outage Probability for D_f

$$P_{out}^{D_f} = 1 - \Pr\left(\min\left(\frac{\gamma_{x_1}^{SR}}{\gamma_{thf}}, \frac{\gamma_{x_2}^{SR}}{\gamma_{thn}}, \frac{\gamma_{x_1}^{RD_f}}{\gamma_{thf}}\right) > 1\right)$$

$$= 1 - \underbrace{\Pr\left(\gamma_{x_1}^{SR} > \gamma_{thf}, \gamma_{x_2}^{SR} > \gamma_{thn}\right)}_{I_1} \underbrace{\Pr\left(\gamma_{x_1}^{RD_f} > \gamma_{thf}\right)}_{I_2}. \tag{A.1}$$

Substituting (7) and (8) into (A1), then the I_1 can be written as:

$$\begin{aligned} I_1 &= \Pr\left(\gamma_{x_1}^{SR} > \gamma_{thf}, \gamma_{x_2}^{SR} > \gamma_{thn}\right) \\ &= \Pr\left(\rho_1 > M_1, \rho_1 > M_2\right) \\ &= 1 - F_{\rho_1}(M_3) \\ &= e^{-\frac{M_3}{\beta_1}}. \end{aligned} \tag{A.2}$$

Substituting (13) into (A1), the I_2 of following expression can be written as

$$\begin{aligned} I_2 &= \Pr\left(\gamma_{x_1}^{RD_f} > \gamma_{thf}\right) \\ &= \Pr\left(\frac{b_1\rho_2\gamma_2 A_2}{b_2\rho_2\gamma_2 A_2 + \rho_2\gamma_2 B_2 + C_2} > \gamma_{thf}\right) \\ &= 1 - F_{\rho_2}(M_4) \\ &= e^{-\frac{M_4}{\beta_2}}. \end{aligned} \tag{A.3}$$

Substituting the expressions of I_1 and I_2 into (A1), the (21) can be obtained.

2) Outage Probability for D_n

$$\begin{aligned} &P_{out}^{D_n} \\ &= \Pr\left(\min\left(\frac{\gamma_{x_1}^{SR}}{\gamma_{thf}}, \frac{\gamma_{x_2}^{SR}}{\gamma_{thn}}\right) < 1\right) \\ &\quad + \Pr\left(\min\left(\frac{\gamma_{x_1}^{SR}}{\gamma_{thf}}, \frac{\gamma_{x_2}^{SR}}{\gamma_{thn}}\right) > 1, \min\left(\frac{\gamma_{x_1}^{RD_n}}{\gamma_{thf}}, \frac{\gamma_{x_2}^{RD_n}}{\gamma_{thn}}\right) < 1\right) \\ &= 1 - \underbrace{\Pr\left(\min\left(\frac{\gamma_{x_1}^{SR}}{\gamma_{thf}}, \frac{\gamma_{x_2}^{SR}}{\gamma_{thn}}\right) > 1\right)}_{I_3} \\ &\quad + \Pr\left(\min\left(\frac{\gamma_{x_1}^{SR}}{\gamma_{thf}}, \frac{\gamma_{x_2}^{SR}}{\gamma_{thn}}\right) > 1\right) \underbrace{\Pr\left(\min\left(\frac{\gamma_{x_1}^{RD_n}}{\gamma_{thf}}, \frac{\gamma_{x_2}^{RD_n}}{\gamma_{thn}}\right) < 1\right)}_{I_4}, \end{aligned} \tag{A.4}$$

where

$$\begin{aligned} I_3 &= \Pr\left(\min\left(\frac{\gamma_{x_1}^{SR}}{\gamma_{thf}}, \frac{\gamma_{x_2}^{SR}}{\gamma_{thn}}\right) > 1\right) \\ &= \Pr\left(\gamma_{x_1}^{SR} > \gamma_{thf}, \gamma_{x_2}^{SR} > \gamma_{thn}\right) \\ &= I_1. \end{aligned} \tag{A.5}$$

Substituting (14) and (15) into (A4), then the I_4 can be written as

$$I_4 = \Pr\left(\min\left(\frac{\gamma_{x_1}^{RD_n}}{\gamma_{thf}}, \frac{\gamma_{x_2}^{RD_n}}{\gamma_{thn}}\right) < 1\right)$$

$$= 1 - \Pr\left(\gamma_{x_1}^{RD_n} > \gamma_{thf}, \gamma_{x_2}^{RD_n} > \gamma_{thn}\right)$$
$$= e^{-\frac{M_7}{\beta_3}}. \quad \text{(A.6)}$$

Substituting the expressions of I_3 and I_4 into (A4), the (25) can be obtained.

APPENDIX B: PROOF OF THEOREM 1

Intercept Probability for D_f

$$P_{int}^{D_f} = \Pr\left(\gamma_{x_1}^{SR} > \gamma_{thf}, \gamma_{x_2}^{SR} > \gamma_{thn}, \gamma_{x_1}^{RE} > \gamma_{thE_1}\right)$$
$$= \Pr\left(\gamma_{x_1}^{SR} > \gamma_{thf}, \gamma_{x_2}^{SR} > \gamma_{thn}\right) \underbrace{\Pr\left(\gamma_{x_1}^{RE} > \gamma_{thE_1}\right)}_{I_5}$$
$$= e^{-\left(\frac{D_3}{\beta_{SR}} + \frac{E_1}{\beta_{RE}}\right)}. \quad \text{(A.7)}$$

Substituting (16) into (B1), then the I_5 can be written as $I_5 = e^{-\frac{N_1}{\beta_4}}$. Similarly, we can also obtain the IP for D_n.

REFERENCES

[1] M. Alkhawatrah, Y. Gong, G. Chen, S. Lambotharan, and J. A. Chambers, "Buffer-aided relay selection for cooperative NOMA in the Internet of Things," *IEEE Internet Things J.*, vol. 6, no. 3, pp. 5722–5731, Jun. 2019.

[2] D. Zhang, Y. Liu, Z. Ding, Z. Zhou, A. Nallanathan, and T. Sato, "Performance analysis of non-regenerative Massive-MIMO-NOMA relay systems for 5G," *IEEE Trans. Commun.*, vol. 65, no. 11, pp. 4777–4790, Nov. 2017.

[3] X. Li, J. Li, and L. Li, "Performance analysis of impaired SWIPT NOMA relaying networks over imperfect weibull channels," *IEEE Syst. J.*, vol. 14, no. 1, pp. 669–672, Mar. 2020.

[4] J. Men, J. Ge, and C. Zhang, "Performance analysis of nonorthogonal multiple access for relaying networks over nakagami-*m* fading channels," *IEEE Trans. Veh. Technol.*, vol. 66, no. 2, pp. 1200–1208, Feb. 2017.

[5] J. Men, J. Ge, and C. Zhang, "Performance analysis for downlink relaying aided non-orthogonal multiple access networks with imperfect CSI over nakagami-*m* fading," *IEEE Access*, vol. 5, pp. 998–1004, 2017.

[6] Z. Zhou, H. Yu, C. Xu, Y. Zhang, S. Mumtaz, and J. Rodriguez, "Dependable content distribution in D2D-based cooperative vehicular networks: A big data-integrated coalition game approach," *IEEE Trans. Intell. Transp. Syst.*, vol. 19, no. 3, pp. 953–964, Mar. 2018.

[7] Z. Ding, M. Peng, and H. V. Poor, "Cooperative non-orthogonal multiple access in 5G systems," *IEEE Commun. Lett.*, vol. 19, no. 8, pp. 1462–1465, Aug. 2015.

[8] Q. Y. Liau and C. Y. Leow, "Successive user relaying in cooperative NOMA system," *IEEE Wireless Commun. Lett.*, vol. 8, no. 3, pp. 921–924, Jun. 2019.

[9] L. Lv, J. Chen, Q. Ni, Z. Ding, and H. Jiang, "Cognitive non-orthogonal multiple access with cooperative relaying: A new wireless frontier for 5G spectrum sharing," *IEEE Commun. Mag.*, vol. 56, no. 4, pp. 188–195, Apr. 2018.

[10] B. Ning, W. Hao, A. Zhang, J. Zhang, and G. Gui, "Energy efficiency–delay tradeoff for a cooperative NOMA system," *IEEE Commun. Lett.*, vol. 23, no. 4, pp. 732–735, Apr. 2019.

[11] O. Abbasi, A. Ebrahimi, and N. Mokari, "NOMA inspired cooperative relaying system using an AF relay," *IEEE Wireless Commun. Lett.*, vol. 8, no. 1, pp. 261–264, Feb. 2019.

[12] S. M. Ibraheem, W. Bedawy, W. Saad, and M. Shokair, "Outage performance of NOMA-based DF relay sharing networks over Nakagami-m fading channels," in *Proc. 13th Int. Conf. Comput. Eng. Syst. (ICCES)*, Dec. 2018, pp. 512–517.

[13] X. Li, M. Huang, C. Zhang, D. Deng, K. M. Rabie, Y. Ding, and J. Du, "Security and reliability performance analysis of cooperative multi-relay systems with nonlinear energy harvesters and hardware impairments," *IEEE Access*, vol. 7, pp. 102644–102661, 2019.

[14] Z. Zhou, X. Chen, Y. Zhang, and S. Mumtaz, "Blockchain-empowered secure spectrum sharing for 5G heterogeneous networks," *IEEE Netw.*, vol. 34, no. 1, pp. 24–31, Jan. 2020.

[15] A. D. Wyner, "The wire-tap channel," *Bell Syst. Tech. J.*, vol. 54, no. 8, pp. 1355–1387, Oct. 1975.

[16] P. Ngoc Son and H. Yun Kong, "Performance analysis of a decode-and-forward scheme under physical layer security over rician fading channel," in *Proc. Int. Conf. ICT Converg. (ICTC)*, Oct. 2013, pp. 348–352.

[17] Y. Huang, P. Zhang, Q. Wu, and J. Wang, "Secrecy performance of wireless powered communication networks with multiple eavesdroppers and outdated CSI," *IEEE Access*, vol. 6, pp. 33774–33788, 2018.

[18] N. Zaghdoud, W. H. Alouane, H. Boujemaa, and F. Touati, "Secure performance of AF and DF relaying in cooperative noma systems," in *Proc. 19th Int. Conf. Sci. Techn. Autom. Control Comput. Eng. (STA)*, Mar. 2019, pp. 614–619.

[19] C. Yuan, X. Tao, N. Li, W. Ni, R. P. Liu, and P. Zhang, "Analysis on secrecy capacity of cooperative non-orthogonal multiple access with proactive jamming," *IEEE Trans. Veh. Technol.*, vol. 68, no. 3, pp. 2682–2696, Mar. 2019.

[20] B. Li, X. Qi, K. Huang, Z. Fei, F. Zhou, and R. Q. Hu, "Security-reliability tradeoff analysis for cooperative NOMA in cognitive radio networks," *IEEE Trans. Commun.*, vol. 67, no. 1, pp. 83–96, Jan. 2019.

[21] H. Lei, Z. Yang, K.-H. Park, I. S. Ansari, Y. Guo, G. Pan, and M.-S. Alouini, "Secrecy outage analysis for cooperative NOMA systems with relay selection schemes," *IEEE Trans. Commun.*, vol. 67, no. 9, pp. 6282–6298, Sep. 2019.

[22] Y. Feng, S. Yan, C. Liu, Z. Yang, and N. Yang, "Two-stage relay selection for enhancing physical layer security in non-orthogonal multiple access," *IEEE Trans. Inf. Forensics Secur.*, vol. 14, no. 6, pp. 1670–1683, Jun. 2019.

[23] S. Goel and R. Negi, "Guaranteeing secrecy using artificial noise," *IEEE Trans. Wireless Commun.*, vol. 7, no. 6, pp. 2180–2189, Jun. 2008.

[24] Y. Liu, Z. Qin, M. Elkashlan, Y. Gao, and L. Hanzo, "Enhancing the physical layer security of non-orthogonal multiple access in large-scale networks," *IEEE Trans. Wireless Commun.*, vol. 16, no. 3, pp. 1656–1672, Mar. 2017.

[25] A.-A.-A. Boulogeorgos, V. M. Kapinas, R. Schober, and G. K. Karagiannidis, "I/Q-imbalance self-interference coordination," *IEEE Trans. Wireless Commun.*, vol. 15, no. 6, pp. 4157–4170, Jun. 2016.

[26] S. A. Bassam, S. Boumaiza, and F. M. Ghannouchi, "Block-wise estimation of and compensation for I/Q imbalance in direct-conversion transmitters," *IEEE Trans. Signal Process.*, vol. 57, no. 12, pp. 4970–4973, Dec. 2009.

[27] O. Ozdemir, R. Hamila, and N. Al-Dhahir, "Exact average OFDM subcarrier SINR analysis under joint transmit–receive I/Q imbalance," *IEEE Trans. Veh. Technol.*, vol. 63, no. 8, pp. 4125–4130, Oct. 2014.

[28] J. Li, M. Matthaiou, and T. Svensson, "I/Q imbalance in AF dual-hop relaying: Performance analysis in Nakagami-*m* fading," *IEEE Trans. Commun.*, vol. 62, no. 3, pp. 836–847, Mar. 2014.

[29] L. Chen, A. G. Helmy, G. Yue, S. Li, and N. Al-Dhahir, "Performance analysis and compensation of joint TX/RX I/Q imbalance in differential STBC-OFDM," *IEEE Trans. Veh. Technol.*, vol. 66, no. 7, pp. 6184–6200, Jul. 2017.

[30] R. Hamila, O. Ozdemir, and N. Al-Dhahir, "Beamforming OFDM performance under joint phase noise and I/Q imbalance," *IEEE Trans. Veh. Technol.*, vol. 65, no. 5, pp. 2978–2989, May 2016.

[31] P. Hao, X. Wang, and A. Behnad, "Relay authentication by exploiting I/Q imbalance in amplify-and-forward system," in *Proc. IEEE Global Commun. Conf.*, Dec. 2014, pp. 613–618.

[32] B. Selim, S. Muhaidat, P. C. Sofotasios, B. S. Sharif, T. Stouraitis, G. K. Karagiannidis, and N. Al-Dhahir, "Performance analysis of non-orthogonal multiple access under I/Q imbalance," *IEEE Access*, vol. 6, pp. 18453–18468, 2018.

[33] X. Tian, Q. Li, X. Li, H. Peng, C. Zhang, K. M. Rabie, and R. Kharel, "I/Q imbalance and imperfect SIC on two-way relay NOMA systems," *Electronics*, vol. 9, no. 2, pp. 1–16, Feb. 2020.

[34] T. Schenk, *RF Imperfections in High-Rate Wireless Systems*. Berlin, Germany: Springer, 2008.

[35] X. Li, M. Liu, C. Deng, P. T. Mathiopoulos, Z. Ding, and Y. Liu, "Full-duplex cooperative NOMA relaying systems with I/Q imbalance and imperfect SIC," *IEEE Wireless Commun. Lett.*, vol. 9, no. 1, pp. 17–20, Jan. 2020.
[36] J. Qi, S. Aissa, and M.-S. Alouini, "Impact of I/Q imbalance on the performance of two-way CSI-assisted AF relaying," in *Proc. IEEE Wireless Commun. Netw. Conf. (WCNC)*, Apr. 2013, pp. 2507–2512.
[37] M. Li, B. Selim, S. Muhaidat, P. C. Sofotasios, M. Dianati, P. D. Yoo, J. Liang, and A. Wang, "Effects of residual hardware impairments on secure NOMA-based cooperative systems," *IEEE Access*, vol. 8, pp. 2524–2536, 2020.

XINGWANG LI (Senior Member, IEEE) received the B.Sc. degree from Henan Polytechnic University, in 2007, the M.Sc. degree from the University of Electronic Science and Technology of China, in 2010, and the Ph.D. degree from the Beijing University of Posts and Telecommunications, in 2015. From 2010 to 2012, he was working with Comba Telecom Ltd., Guangzhou, China, as an Engineer. From 2017 to 2018, he was a Visiting Scholar with Queen's University Belfast, Belfast, U.K. He is currently an Associate Professor with the School of Physics and Electronic Information Engineering, Henan Polytechnic University, Jiaozuo, China. His research interests include MIMO communication, cooperative communication, hardware constrained communication, non-orthogonal multiple access, physical layer security, unmanned aerial vehicles, and the Internet-of-Things.

He is currently an Editor on the Editorial Board of IEEE Access, *Computer Communications*, *Physical Communication*, and *KSII Transactions on Internet and Information Systems*. He is also a Lead Guest Editor of the special issue on Recent Advances in Physical Layer Technologies for 5G-Enabled Internet of Things of Wireless Communications and Mobile Computing. He has served as many TPC/Co-Chair, such as IEEE GLOBECOM, IEEE/CIC ICCC, IEEE WCNC, IEEE VTC, and IEEE/IET CSNDSP.

MENGLE ZHAO received the B.Sc. degree in electronic information engineering with the School of Physics and Electronic Information Engineering, Henan Polytechnic University, Jiaozuo, China, in 2018, where she is currently pursuing the M.Sc. degree in communication and information systems with the School of Physics and Electronic Information Engineering. Her current research interests include non-orthogonal multiple access, physical layer security, in-phase and quadrature-phase imbalance, cooperative communication, and backscatter device.

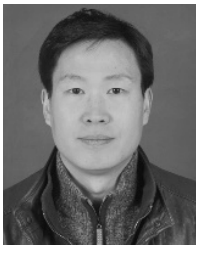

XIANG-CHUAN GAO received the B.Sc. and M.Eng. degrees from Zhengzhou University, Zhengzhou, China, in 2005 and 2008, respectively, and the Ph.D. degree from the Beijing University of Posts and Telecommunications, Beijing, China, in 2011. His current research interests include massive MIMO, cooperative communications, and visible light communication.

LIHUA LI received the Ph.D. degree from the Beijing University of Posts and Telecommunications (BUPT), in 2004. She had been a short-term Visiting Scholar with Brunel University, U.K., in 2006. She visited the University of Oulu, from August 2010 to August 2011. She is currently an Associate Professor with BUPT. She has published 63 articles in international and domestic journals and academic conferences, and five books. She has applied 20 national invention patents and one international patent. She was selected and funded as one of the New Century Excellent Talents by the Chinese Ministry of Education, in 2008. Her research focuses on wideband mobile communication technologies including MIMO, link adaptation, and cooperative transmission technologies, relating to new generation mobile communication systems such as LTE and IMT-Advanced. She received the First Prize of the China Institute of Communications Science and Technology Award, in 2006, for her research achievements of Wideband Wireless Mobile TDD-OFDM-MIMO Technologies, and the Second Prize of China State Technological Invention Award (the first level award in China), in 2008. She has served as a Group Leader for 3GPP LTE RAN1 standardization work on behalf of BUPT, in 2005, when she submitted more than 20 relevant proposals to 3GPP LTE and seven of them were accepted. She has been taking part in China IMT-Advanced technology Work Group, since 2007. So far she has submitted 33 relevant proposals, 15 of which were accepted.

DINH-THUAN DO (Senior Member, IEEE) received the B.S., M.Eng., and Ph.D. degrees from Vietnam National University (VNU-HCMC), in 2003, 2007, and 2013, respectively, all in communications engineering. He was a Senior Engineer with VinaPhone Mobile Network, from 2003 to 2009. He was a Visiting Ph.D. Student with the Communications Engineering Institute, National Tsing Hua University, Taiwan, from 2009 to 2010. His name and his achievements will be reported in special book entitle *Young Talents in Vietnam 2015-2020*. His publications include over 53 SCIE/SCI-indexed journal articles, more than 45 SCOPUS-indexed journal articles and more than 50 international conference papers. He is a sole author of one textbook and one book chapter. His research interests include signal processing in wireless communications network, NOMA, full-duplex transmission, and energy harvesting. He was a recipient of the Golden Globe Award from the Vietnam Ministry of Science and Technology, in 2015 (Top 10 most excellent scientist nationwide). He is currently serving as an Editor for *Computer Communications* (Elservier), an Associate Editor for *EURASIP Journal on Wireless Communications and Networking* (Springer), and an Editor for *KSII Transactions on Internet and Information Systems*.

KHALED M. RABIE (Member, IEEE) received the B.Sc. degree (Hons.) in electrical and electronic engineering from the University of Tripoli, Tripoli, Libya, in 2008, and the M.Sc. and Ph.D. degrees in communication engineering from The University of Manchester, Manchester, U.K., in 2010 and 2015, respectively. He is currently a Postdoctoral Research Associate with Manchester Metropolitan University (MMU), Manchester. His research interests include signal processing and the analysis of power line and wireless communication networks. He is a Fellow of the U.K. Higher Education Academy. He was a recipient of the Best Student Paper Award at the IEEE ISPLC, TX, USA, 2015, and the MMU Outstanding Knowledge Exchange Project Award, in 2016. He is currently the Program Chair of the IEEE ISPLC 2018 and the IEEE CSNDSP 2018, the Co-Chair of the Green Communications and Networks track, and the Publicity Chair of the INISCOM 2018. He is also an Associate Editor of IEEE Access, and an Editor of the *Physical Communication* journal (Elsevier).

RUPAK KHAREL (Senior Member, IEEE) received the Ph.D. degree in secure communication systems from Northumbria University, U.K., in 2011. He is currently a Senior Lecturer with the School of Engineering, Manchester Metropolitan University. His research interests include various use cases and the challenges of the IoT and cyber physical systems (CPS), cyber security challenges on CPS, the energy optimization of the IoT networks forgreen computing, the Internet of Connected Vehicles (IoV), and smart infrastructure systems. He is a Principal Investigator of multiple government and industry funded research projects. He is a member of the IET and a Fellow of the Higher Education Academy (FHEA), U.K.